Application of the Rheological Model to the Creep Analysis Coupled with Plastic Deformation

S.H. Lee
The MacNeal-Schwendler Corporation, 815 West Colorado Blvd., Los Angeles, California 90041, U.S.A.

Abstract

A creep analysis capability, introduced for general purpose finite element analysis, is described. State-of-the-art theory and algorithms are employed to process the creep behavior coupled with elastoplastic deformation at elevated temperatures. The formulation is based on the step-by-step time-integration of the Kelvin-Maxwell rheological model.

The concept of a rheological model is extended to the multiaxial stresses by the Prandtl-Reuss stress-strain relationship, from which the tangential stiffness matrix is formed for Newton's iteration. If the plastic deformation is coupled with creep, the material routine will seek a solution in two distinct steps. Various choices of empirical creep laws are available and small variations in temperature are allowed.

1. Introduction

A specimen subjected to a constant uniaxial tension at an elevated temperature exhibits three distinct phases in a time frame: primary creep stage, secondary creep stage and the tertiary creep stage to rupture. If the specimen is unloaded after some creep deformation, the elastic strain is immediately recovered and a portion of the creep strain is gradually recovered. The recoverable portion of the creep deformation is called primary creep and the non-recoverable portion, secondary creep. The tertiary creep, similar to necking in plasticity, is considered as a localized instability phenomenon, which is beyond the scope of this paper.

Elaborating on the Kelvin-Maxwell rheological creep model developed by Badani[1], the creep behavior can be coupled with plastic deformation. The Kelvin element describes the primary creep behavior and the Maxwell element represents the secondary creep. For a generalization of the viscoelastic material behavior, the rheological model parameters are treated as nonlinear functions of the effective stress and the temperature. The step-by-step integration is performed using the central difference method assuming that the rheological model parameters remain constant for a short time interval.

A number of empirical creep laws, recommended by the Oak Ridge National Laboratory (ORNL), are provided along with options for general tabular input. When the creep characteristics are specified in terms of empirical creep laws, the program converts the empirical formula to the corresponding rheological model.

2. Effects of Stress and Temperature on the Creep Rate

An analytical solution to the Kelvin-Maxwell model subjected to a constant stress (σ) is given by

$$\varepsilon^c_{total} = \frac{\sigma}{C_s} t + \varepsilon^c_{primary} \quad (1)$$

where

$$\varepsilon^c_{primary} = \frac{\sigma}{K_p}[1 - e^{-(K_p/C_p)t}] \quad .$$

For a varying stress case, however, an instantaneous strain-rate should be considered to have the creep hardening effects. The creep hardening (and softening) effects, exhibited by the primary creep, are accounted for by using the creep hardening law, wherein creep strain rates are expressed in terms of primary creep strain rather than time, i.e.

$$\dot{\varepsilon}^c_{total} = \frac{\sigma}{C_s} + \dot{\varepsilon}^c_{primary} \quad (2)$$

where

$$\dot{\varepsilon}^c_{primary} = \frac{1}{C_p}(\sigma - K_p\, \varepsilon^c_{primary}) \quad .$$

The creep strain rate is also a function of the absolute temperature. Microscopically, the creep deformation is an integrated effect of dislocations of the crystal structure primarily due to thermal activation and stress. The effects of temperature at the microscopic level can be quantified as

$$\dot{\varepsilon}^c = A\, e^{-\Delta H/RT} \quad (3)$$

where ΔH is the energy of activation, R is the constant, T is the absolute temperature and A is in strain/unit time. On this basis, the creep model parameters measured at a reference temperature T_0 can be used to compute the creep strain rate at the temperature T in the vicinity of T_0, allowing small variations in the ambient temperature. The creep model parameters are corrected as

$$C_s(T) = \frac{C_s(T_0)}{F_c} \quad \text{and} \quad C_p(T) = \frac{C_p(T_0)}{F_c} \quad (4)$$

where

$$F_c = \frac{\dot{\varepsilon}^c}{\dot{\varepsilon}^c_0} = (e^{-\Delta H/RTo})^{(\frac{T_0}{T} - 1)} \quad .$$

3. Equilibrium Consideration for a Deviatoric Stress Component

Suppose that the Kelvin-Maxwell model is applied to a typical deviatoric stress component. Referring to Figure 1, the state equilibrium equation of the model at any instant is expressed as:

$$[C]\{\Delta\dot{e}\} + [K]\{\Delta e\} = \{\Delta s\} \quad (5)$$

where

$$[C] = \begin{bmatrix} C_s & -C_s \\ -C_s & (C_p + C_s) \end{bmatrix}, \quad [K] = \begin{bmatrix} 0 & 0 \\ 0 & K_p \end{bmatrix}, \quad \{\Delta s\}^T = \langle \Delta s_1 \quad 0 \rangle \quad .$$

Introducing the central difference method for the strain-rate increment $(\Delta\dot{e})$, Eq. (5) may be reduced to

$$[\frac{2}{\Delta t} C + K]\{\Delta e\} = 2[C]\{\dot{e}\} + \{\Delta s\} \quad . \quad (6)$$

Defining the stiffness of the primary and secondary creep elements by

$$k_1 = k_p + \frac{2C_p}{\Delta t} \quad \text{and} \quad k_2 = \frac{2C_s}{\Delta t} \quad (7)$$

the equivalent creep stiffness for a deviatoric stress-strain pair can be determined by

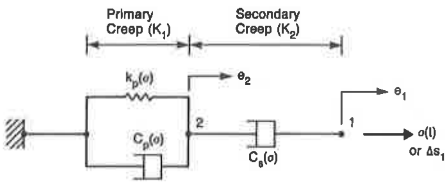

Figure 1. Rheological Model.

$$k_c = \frac{k_1 k_2}{k_1 + k_2} \quad . \tag{8}$$

Solving Eq. (6) for Δe_1 gives

$$k_c \Delta e_1 = \Delta s' + \Delta s_1 \tag{9}$$

where $\Delta s'$ is a pseudo incremental stress, i.e.

$$\Delta s' = 2\left[\frac{C_s}{k_2}(\dot{e}_1 - \dot{e}_2) + \frac{C_p}{k_1} e_2\right]k_c \tag{10}$$

The pseudo incremental stress represents the change in deviatoric stress component due to creep relaxation. This value of $\Delta s'$ can be converted to the equivalent psuedo incremental strain $\Delta e'$, which represents the change in deviatoric strain component due to creep. By virtue of creep volume constancy, deviatoric strains ($\Delta e'$) and the strain rates ($\dot{e}_1$ and $\dot{e}_2$) in Eq. (10) are identical to the ordinary strain components. Hence $\Delta e'$ can be expressed as

$$\Delta\varepsilon' = \frac{\Delta s'}{k_c} = 2\left[\frac{C_s}{k_2}(\dot{\varepsilon}_1 - \dot{\varepsilon}_2) + \frac{C_p}{k_1}\dot{\varepsilon}_2\right] \quad . \tag{11}$$

4. <u>Formation of Tangential Stiffness</u>

The concept of the rheological model for a stress-strain pair is extended to the general multiaxial stresses by adopting the Prandtl-Reuss stress-strain relationship, i.e.

$$\{\dot{\varepsilon}^c\} = \frac{3}{2}\,\frac{\dot{\bar{\varepsilon}}^c}{\bar{\sigma}}\{s\} \tag{12}$$

where creep strain rates $\{\dot{\varepsilon}^c\}^T = < \dot{\varepsilon}^c_x \ \dot{\varepsilon}^c_y \ \dot{\varepsilon}^c_z \ \ \dot{\tau}^c_{xy} \ \dot{\tau}^c_{yz} \ \dot{\tau}^c_{zx} >$,

deviatoric stresses $\{s\}^T = < \sigma'_x \ \sigma'_y \ \sigma'_z \ \ 2\tau_{xy} \ 2\tau_{yz} \ 2\tau_{zx} >$,

and the effective stress ($\bar{\sigma}$) and the effective creep strain rate ($\dot{\bar{\varepsilon}}^c$) are defined identical to those in plasticity with von Mises yield criterion. Implied by this relationship, there is a unique set of rheological parameters ($\bar{K}_p$, $\bar{C}_p$ and $\bar{C}_s$) based on the effective stress, which can be related to all the deviatoric stress components and the corresponding creep strain rates. In terms of effective creep model parameters, Eqs. (7) and (11) may be rewritten as follows:

$$k_1 = \frac{2}{3}\left(\bar{K}_p + \frac{2\bar{C}_p}{\Delta t}\right), \qquad k_2 = \frac{4}{3}\,\frac{\bar{C}_s}{\Delta t} \tag{7a}$$

and

$$\{\Delta\varepsilon'\} = \frac{4}{3}\left[\frac{\bar{C}_s}{k_2}\{\dot{\varepsilon}^c_{total} - \dot{\varepsilon}^c_{primary}\} + \frac{\bar{C}_p}{k_1}\{\dot{\varepsilon}^c_{primary}\}\right] \tag{11a}$$

The creep strain rates in Eq. (2) may be rewritten likewise, i.e., in terms of deviatoric stresses

$$\{\dot{\varepsilon}^c_{total}\} = \frac{3}{2\bar{C}_s}\{s\} + \{\dot{\varepsilon}^c_{primary}\} \tag{2a}$$

where

$$\{\dot{\varepsilon}^c_{primary}\} = \frac{3}{2\bar{C}_p}\{s\} - \frac{\bar{K}_p}{\bar{C}_p}\{\varepsilon^c_{primary}\} \quad .$$

Then the pseudo incremental strain in Eq. (11a) is reduced to

$$\{\Delta\varepsilon'\} = 2\left(\frac{1}{k_1} + \frac{1}{k_2}\right)\{s\} - \frac{4}{3}\,\frac{\bar{K}_p}{k_1}\{\varepsilon^c_{primary}\} \quad . \tag{13}$$

In the absence of plastic deformation, the total strain increment may be expressed as

$$\{\Delta\varepsilon^e + \Delta\varepsilon^c\} = [D_e^{-1} + D_c^{-1}]\ \{\Delta\sigma\} \tag{14}$$

where D_e and D_c are material matrices for elasticity and creep, respectively. However, the total strain increment must be corrected with a pseudo incremental strain vector $\{\Delta\varepsilon'\}$, i.e.,

$$\{\Delta\varepsilon^e + \Delta\varepsilon^c\} = \{\Delta\varepsilon - \Delta\varepsilon'\} \tag{15}$$

Combining Eqs. (14) and (15), we obtain

$$\{\Delta\sigma\} = [D_{ec}]\ \{\Delta\varepsilon - \Delta\varepsilon'\} \tag{16}$$

where $[D_{ec}] = [D_e^{-1} + D_c^{-1}]^{-1}$.

5. Coupling of Plasticity

The plastic strain increment may be obtained by

$$\{\Delta\varepsilon^p\} = D_p^{-1}\ \{\Delta\sigma\} \tag{17}$$

where $D_p^{-1} = \frac{1}{H} \{\frac{\partial f}{\partial \sigma}\} \{\frac{\partial f}{\partial \sigma}\}^T$

with plasticity modulus $H = \frac{d\bar{\sigma}}{d\bar{\varepsilon}^p}$ and the function (f) defining effective stress. Introducing Eq. (17) into Eq. (14), the elasto-plastic-creep stress-strain relations are established as

$$[D_e^{-1} + D_c^{-1} + D_p^{-1}]\ \{\Delta\sigma\} = \{\Delta\varepsilon - \Delta\varepsilon'\} \tag{18}$$

from which the stress increment vector $\{\Delta\sigma\}$ can be obtained. However, Eq. (18) may be rearranged as

$$\{\Delta\sigma\} = [D_{ec}]\ \{\Delta\varepsilon - \Delta\varepsilon'\} - \Delta\lambda[D_{ec}]\ \{\frac{\partial f}{\partial \sigma}\} \tag{19}$$

where $\Delta\lambda = \dfrac{\{\frac{\partial f}{\partial \sigma}\}^T D_{ec}\{\Delta\varepsilon - \Delta\varepsilon'\}}{H + \{\frac{\partial f}{\partial \sigma}\}^T D_{ec}\{\frac{\partial f}{\partial \sigma}\}} \equiv \Delta\bar{\varepsilon}^p > 0$.

The creep deformation tends to relax the stress gradient in the absence of further increments in external loads. In the creep-dominant process, therefore, plastic deformation can only be induced by creep to alleviate stresses in the neighboring material. For this reason, the material routine employs a solution scheme which seeks a solution in two steps when the plastic deformation is coupled with creep. First, it solves for the incremental stress components with an elastic-creep material. Then, if the new stress state exceeds the current yield stress, a correction is made on a previously obtained incremental stresses based on Eq. (19) and the plastic strains are computed.

6. Implementation

A nonlinear static analysis can readily be converted to creep analysis by adding a few creep related data. All the potentially nonlinear elements (RØD, BEAM, QUAD4, TRIA3, HEXA and PENTA) are applicable to creep analysis, but not all the nonlinear elements in the model need to be made with creep material. Users are allowed to either specify an empirical creep law or provide direct input of rheological parameter values as functions of the effective stress. If the creep behavior is prescribed by a creep law, creep law parameters will be converted to rheological parameters whenever a new stress state is computed for the creep analysis. The empirical creep laws provided in MSC/NASTRAN are in the following equation forms with user specified coefficients (a-g):

$$\varepsilon^c(\sigma,t) = a\ \sigma^b t^d \tag{20}$$

and

$$\varepsilon^c(\sigma,t) = A(\sigma)\ [1 - e^{-R(\sigma)t}] + K(\sigma)t \tag{21}$$

for all combinations of types 1 and 2 for A, R and K which are expressed as

Parameter	Type 1	Type 2
$A(\sigma)$	$a\sigma^b$	$a \text{ Exp } (b\sigma)$
$R(\sigma)$	$c \text{ Exp } (d\sigma)$	$c\sigma^d$
$K(\sigma)$	$e[\sinh(f\sigma)]^g$	$e \text{ Exp } (f\sigma)$

The material routine computes the elastic-creep tangential matrix for the formation of a global stiffness matrix, which is used for the modified Newton-Raphson method. Equilibrium condition is guaranteed because the convergence is achieved for every time increment.

The numerical solution scheme employed in the creep formulation is unconditionally stable. However, a limit should be placed on the time increment to achieve an accurate solution. The time increment should be selected so that the strain and/or stress do not change excessively in a single step. Although the extent of excessiveness is problem-dependent, the upper limit is set in the program to issue a warning message.

The total creep strain increment can be recovered by subtracting $\{\Delta\varepsilon^e\}$ and $\{\Delta\varepsilon^p\}$ from total $\{\Delta\varepsilon\}$ in Eq. (18). The primary creep strain increment is saved in the database to take into account creep hardening/softening effects.

7. Verification and Validation

All aspects of creep capabilities were verified with respect to the algorithm, accuracy, and coding errors with a wide variety of problems in MSC/NASTRAN. All types of elements (1D, 2D and 3D) have been tested and known solutions have been reproduced. Various creep laws in the form of Eq. (21) and the direct input of rheological parameters reproduced analytical solutions accurately with errors less than 0.1% in the creep strain at the end of 70 steps. Creep laws in Eq. (20), however, produced a cumulative error of 15-19% in the creep strain at the end of 70 steps, because of the mismatch between the empirical formula and the rheological model.

The creep analysis capability under variable temperatures is verified using empirical creep laws recommended by ORNL. There are two different creep laws (types 111 and 121) for the same material (type 304 stainless steel) established at different temperatures (1100^o F and 1200^o F) as shown in Figure 2. The creep law type 111 represents the creep behavior at 1100^o F. This creep law is applied at the operating temperature of 1200^o F with corrections for variable temperature. The results are compared with the creep law type 121, which predicts proper creep behavior at 1200^o F. The accuracy of the varying temperature case was found satisfactory only for a short period of time or for small temperature variations. Nevertheless this feature is considered useful and essential.

Coupling of the plastic deformation with creep is verified by reproducing the isochronous stress-strain curve for stainless steel, type 304, as shown in Figure 3. The data points are obtained in 15 steps to the creep time of 100 hours. The creep behavior is manifested in the relaxation process under constant strain. Figure 4 compares relaxation predictions by various methods.

The creep response of various elements to the stress reversal was thoroughly investigated. The effects of the creep hardening/softening were exhibited properly.

However, the convergence required a stiffness matrix update and the smaller time increment at the onset of stress reversal.

The solution to the creep behavior of an infinitely long thick-walled cylinder subjected to internal pressure was presented by Greenbaum and Rubinstein[2]. They employed an incompressible material with a simple empirical formula which accounts only for secondary creep, to which an analytical solution exists. MSC/NASTRAN reproduced the solution very accurately using nine HEXA elements with axisymmetric and plane strain boundary conditions.

The creep behavior of a thick-walled pressure vessel with a flat-end closure was also analyzed[2] under an internal pressure of 445 psi with a material obeying an empirical creep law in the form of Eq. (20). A finite element model of the same pressure vessel was analyzed by MSC/NASTRAN using 72 solid elements with 355 active DOFs. Figure 5 shows stress contours at t=3. For a model five times coarser, this solution represents an excellent agreement with that in Reference[2].

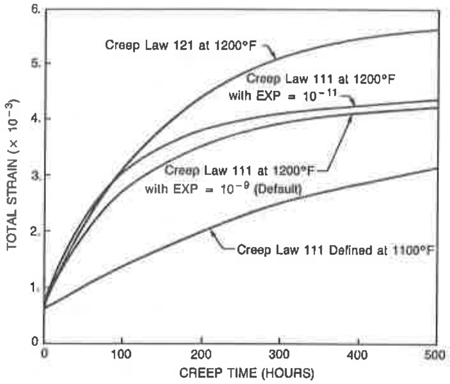

Figure 2. Creep Capability Verification for Variable Temperature.

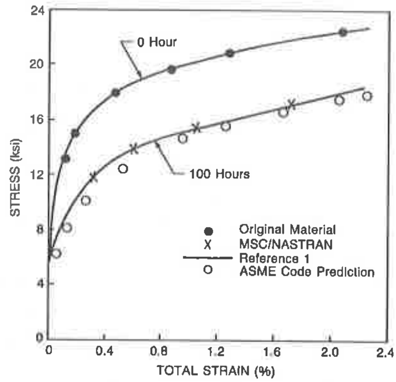

Figure 3. Isochronous Stress-strain Curve.

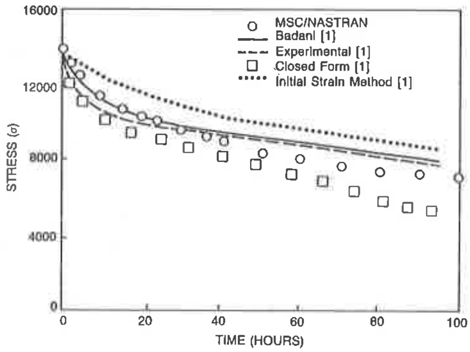

Figure 4. Comparison of Creep Relaxation Predictions.

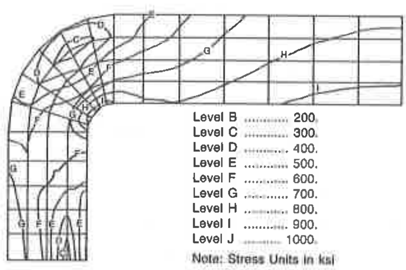

Figure 5. Effective Stress Distribution After 3 Hours of Creep.

8. Nozzle-to-Spherical Shell Attachment as Benchmark Problem

The ORNL's High-Temperature Structural Design(HTSD) program was instigated to develop design methodologies for breeder reactor structures. Under the ORNL program, a nozzle-to-spherical shell attachment model was presented as a benchmark problem with extensive experimental[3] and analytical[4, 5] results. The model represents a liquid-metal fast breeder reacter component, made of type 304 stainless steel, subjected to successive cycles of loading with internal pressure and end moment at 1100^{o} F.

This component is analyzed by MSC/NASTRAN using 1552 DOFs, as shown in Figure 6, with elasto-plastic-creep material and nonlinear geometric effects. The creep characteristics are defined by a creep law in the form of Eq. (21). Typical results at a select point, where the plastic deformation is significant, are compared with data in Reference[4] as shown in Figures 7 and 8. It is noted that MSC/NASTRAN used an isotropic, instead of a kinematic hardening rule as employed by Levy[4]. Figure 9 shows a typical stress contour at t = 2546 hours upon unloading. These results demonstrate a powerful capability of the general purpose program.

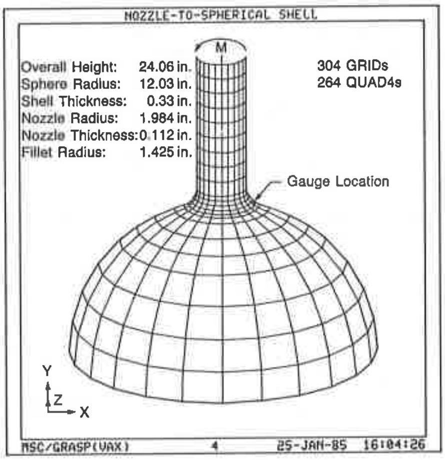

Figure 6. Finite Element Model by MSC/NASTRAN.

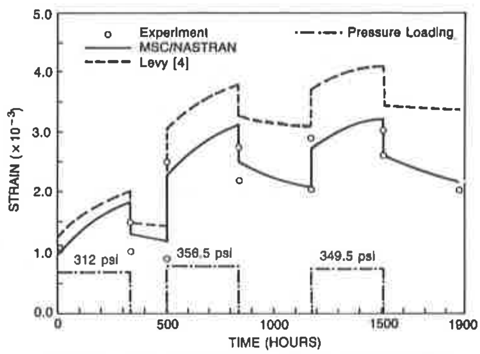

Figure 7. Total Circumferential Strain at Gauge Location During Pressure Loading.

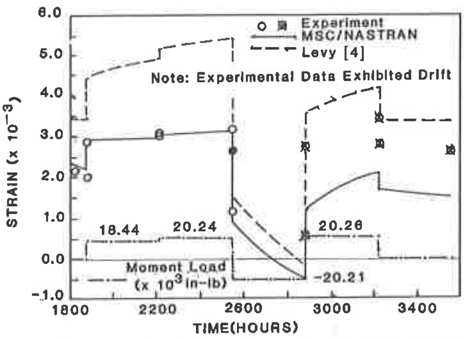

Figure 8. Total Circumferential Strain at Gauge Location During Moment Loading.

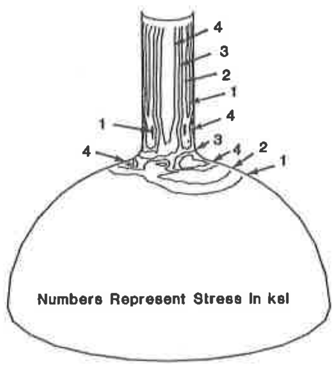

Figure 9. Effective Stress Contour Plot at t = 2546 Hours upon Unloading

9. Concluding Remarks

One of the virtues of the present method is the ability to accommodate stress reversal with ease. Effects of creep hardening and softening were properly reflected in the solution with stress reversal with no special effort.

The creep analysis capability in MSC/NASTRAN is a generalization of the viscoelastic-plastic material capability, applicable to the general 3-dimensional structure. The validity of the theory and the algorithm is proven and the analysis results show close agreement with experimental data. This signifies an introduction of a new dimension and perspective into the general field of nonlinear analysis.

Acknowledgements:

The author wishes to thank Mr. David Herting for encouragements during the creep capability development. He also expresses thanks to Candee Sumner for her assistance in analyzing the nozzle-to-spherical shell attachment model.

References:

[1] BADANI, M. P., "A New Method to Solve Nonlinear Creep Problems in Structural Mechanics Using Incompatible Isoparametric Finite Elements", Ph.D. Dissertation, U. C. Berkeley, 1980.

[2] GREENBAUM, G. A. and RUBINSTEIN, M. F., "Creep Analysis of Axisymmetric Bodies Using Finite Elements", Nuclear Engineering and Design, Vol. 7, 1968.

[3] CLINARD, J. A., et. al., "Elevated-Temperature Deformation and Failure Testing and Analysis of Nozzle-to-Spherical Shells: Specimens NS-2 and NS-1", Oak Ridge National Laboratory, ORNL-5939, January 1983.

[4] LEVY, A. "High-Temperature Inelastic Analysis", Computers and Structures, Vol. 13, 1981.

[5] LEVY, A. and PIFKO, A. B., "On Computational Strategies for Problems Involving Plasticity and Creep", International Journal for Numerical Methods in Engineering, Vol. 17, 1981.

[6] LEE, S. H., "Creep Analysis Capability in MSC/NASTRAN", presented at the MSC/NASTRAN User's Conference, Pasadena, California, March 23, 1984.

[7] ZIENKIEWICZ, O. C., "The Finite Element Method", McGraw-Hill, 1977.

[8] KRAUS, H., "Creep Analysis", John Wiley and Sons, 1980.

[9] POLAKOWSKI, N. H. and RIPLING, E. J., "Strength and Structure of Engineering Materials", Prentice-Hall, 1966.

[10] JUVINALL, R. C., "Stress, Strain and Strength", McGraw-Hill, 1967.